Journal of Electrochemistry

Volume 19
Issue 4 *Special Issue of Environmental Electrochemistry (I) (Editor: Professor LIN Hai-bo)*

2013-08-28

Graphene Quantum Dots Enhanced Electrochemical Performance of Polypyrrole as Supercapacitor Electrode

Kun WU

Si-zhe XU

Xue-jiao ZHOU

Hai-xia WU
Key Laboratory for Thin Film and Microfabrication of the Ministry of Education, Research Institute of Micro/Nano Science and Technology, Shanghai Jiao Tong University, Shanghai 200240, China;,
haixiawu@sjtu.edu.cn

Recommended Citation
Kun WU, Si-zhe XU, Xue-jiao ZHOU, Hai-xia WU. Graphene Quantum Dots Enhanced Electrochemical Performance of Polypyrrole as Supercapacitor Electrode[J]. *Journal of Electrochemistry*, 2013 , 19(4): 361-370.
DOI: 10.61558/2993-074X.2122
Available at: https://jelectrochem.xmu.edu.cn/journal/vol19/iss4/9

Artical ID:1006-3471(2013)04-0361-10

Graphene Quantum Dots Enhanced Electrochemical Performance of Polypyrrole as Supercapacitor Electrode

WU Kun, XU Si-zhe, ZHOU Xue-jiao, WU Hai-xia*

(*Key Laboratory for Thin Film and Microfabrication of the Ministry of Education, Research Institute of Micro/Nano Science and Technology, Shanghai Jiao Tong University, Shanghai* 200240, *China*)

Abstract: With an objective to develop electrode materials with high specific capacitance and good stability, a completely new nanocomposite of Polypyrrole (PPY) and graphene quantum dots (GQD) was successfully obtained through *in-situ* polymerization of pyrrole in the presence of GQD suspension. The obtained composites with different mass ratios were characterized by X-ray diffraction(XRD), Fourier transformed infrared spectroscopy(FT-IR) and scanning electron microscopy (SEM). GQD enhanced electrochemical performance of PPY and, as supercapacitor electrodes, the PPY/GQD composites with the mass ratio of PPY to GQD at 50:1 showed a competitive specific capacitance of 485 $F \cdot g^{-1}$ at a scan rate of 0.005 $V \cdot s^{-1}$. The attenuation of the specific capacitance is about 2% after 2000 cycles. The high specific capacitance and good stability of the PPY/GQD nanocomposites are promising for applications in electrochemical supercapacitors.

Key words: graphene oxide; graphene quantum dots; polypyrrole; supercapacitor

CLC Number: O631; TB332 **Document Code:** A

Environmental pollution and increasing depletion of fossil fuels have created great interest in alternative energy technologies[1-2]. As one of the key technologies to promote the development of renewable energy source, energy storage is always hot spot. Recently, lots of efforts have gone into developing lithium ion batteries and supercapacitors[3-7]. Supercapacitors, which were also called electrochemical capacitors or ultracapacitors[8-9], are energy storage devices between secondary batteries and traditional capacitors. And, because of their longer cycle life, lower cost and better environmental friendliness than secondary batteries[10], supercapacitors have gained much attention over the past decades. With these wonderful advantages, they have been widely used in electrical vehicles, portable electronics and mobile communications[9-11].

In general, supercapacitors possess two energy storage mechanisms: the electrical double-layer capacitance (EDLC) and the pseudocapacitance. The energy in EDLC is stored using ion adsorption, while the energy in pseudocapacitance can be stored by fast surface redox reactions[12-13]. In any case, their excellent properties are greatly depend on the electrode materials, and the ideal electrode material for supercapacitors should have high electrical conductivity, good stability, and exceptional capacity[14]. Porous carbon materials[15] and conducting polymers, such as polyaniline (PANI)[16-17], polypyrrole (PPY)[18-19] and polythiophene (PTH)[20], have been employed as electrode materials of supercapacitors. PPY, with a high electrical conductivity and good mechanical strength, is a promising electrode material for supercapacitors. However, their poor processing property and lower stability restrict their further applications. Therefore, modification of the conductive polymers with carbon

Received: 2012-08-16, Revised: 2012-10-09 *Corresponding author, Tel: (86-21)34206233, E-mail: haixiawu@sjtu.edu.cn
This work was supported by the National Natural Science Foundation of China (No. 20906055), National "973 Program" (No. 2010CB933900), and the State Key Laboratory of Bioreactor Engineering (No. 2060204).

materials is the traditional way. Graphene, a single-atom-thick two-dimensional graphitic carbon material, is a basic building block for graphitic materials of all other dimensionalities and has attracted intense interest because of its extraordinary electrical conductivity and chemical stability[21]. But, graphene tends to aggregate in applications, thus it is a good solution to use the synergies of PPY and graphene to solve the problem. Therefore, many researchers focus their study on graphene/polypyrrole composites.

Bose et al modified polypyrrole with graphene, and they gained electrodes with a high specific capacitance of 267 $F \cdot g^{-1}$ at the scan rate of 0.1 $V \cdot s^{-1}$. However, the composite retains only 90% of specific capacitance just after 500 cycles[14]. Zhang et al also synthesized graphene/polypyrrole composites and made them into electrodes. They found that the specific capacitance was 482 $F \cdot g^{-1}$ at a current density of 0.5 $A \cdot g^{-1}$[10]. In our previous work, we have synthesized layered polypyrrole/chemically reduced graphene oxide (PPY/CRGO) nanocomposites as supercapacitor electrodes through *in-situ* polymerization of pyrrole on graphene oxide (GO) sheets[22]. The electrochemical performance of the composite is excellent with capacitance of 421 $F \cdot g^{-1}$ which could be further increased to 509 $F \cdot g^{-1}$ by introducing pores into it. However, the introduction of pores not only reduced the mechanical properties, but also took much more time. Meanwhile, the cycle stability of the electrodes of above work is all somewhat lower, which may be brought about by the defects of the graphene oxide. These defects have several types and it is still difficult to explain their formation. These defects could decrease the electrical conductivity and even the capacitive behavior[23]. But, perfect graphene oxide can hardly be gained through the oxidization and exfoliation of bulk graphite. Therefore, in order to solve this problem, we cut the graphene oxide into graphene quantum dots along the defects by Photo-Fenton reaction to increase its electrical conductivity by decreasing the defects. An article recently published on-line from our group proved that GQD prepared by this method really have fewer defects[24]. Then, the nanocomposites of polypyrrole (PPY) and graphene quantum dots (GQD) may have better stability and even higher specific capacitance.

In this paper, the composites of PPY and GQD are synthesized simply by *in-situ* polymerization of pyrrole monomer in the presence of GQD suspension. The high specific capacitance of 485 $F \cdot g^{-1}$ is obtained at a scan rate of 0.005 $V \cdot s^{-1}$ and the attenuation of the specific capacitance is about 2% after 2000 cycles at the scan rate of 0.05 $V \cdot s^{-1}$, which indicates that the cycle performance of the electrode was greatly increased. Thus, the new nanocomposites have a better electrochemical performance with the help of GQD and will be ideal electrode materials for supercapacitors.

1 Experimental

1.1 Materials

Natural graphite (crystalline powders, ~ 500 mesh) was acquired from Shanghai Yifan Company (Shanghai, China). Pyrrole monomer, ammonium persulfate(APS), $NaNO_3$ and $KMnO_4$ were purchased from Sinopharm Chemical Reagent Co. Ltd. HCl and H_2SO_4, ethanol were gained from Shanghai Lingfeng Chemical Reagent Co. Ltd. (Shanghai, China). Graphene oxide (GO) was prepared by the modified Hummers method[25-26].

1.2 Preparation of PPY/GQD Composites and Electrodes

PPY/GQD composites (PGQD) were prepared through *in-situ* polymerization of pyrrole in the presence of GQD suspension. First, Graphene Quantum Dots (GQD) was obtained by Photo-Fenton reaction of GO. 25 mL of 1 $mg \cdot mL^{-1}$ GO was mixed with 2 mL H_2O_2 in a 40 mL quartz tube. Then the quartz tube was put in the photocatalytic equipment for 1 h under 1000 watts light of mercury lamp. In this way, we got GQD with the average size of 50 nm and good dispersion. To remove impurities, the pyrrole monomer was pre-purified by distillation under vacuum. Typically, 100 mg (104 μL) of purified pyrrole monomer was added into the 40 mL GQD suspension of 0.05 $mg \cdot mL^{-1}$, then stirred for 30 min in an ice

bath about 0 ~ 2 °C. In the process, the pyrrole monomer was adsorbed onto the surface of GQD. Then 10 mL of APS (34wt%, mole ratio of pyrrole: APS = 1:1) was slowly added into mixture. The polymerization started in 5 ~ 6 min later, and it could be observed that the above mixture turned from transparent to black. Finally, the nanocomposites were obtained after another 30 min stirration. The obtained product was filtered and washed with ethanol and distilled water each for 3 times, and then dried at 40 °C in a vacuum oven for 8 h. The dry powder was named as PGQD50.

To get optimum ratio of composites, we also prepared the composites with pyrrole to GQD mass ratios of 200:1,100:1, 30:1, 20:1, 10:1 and 5:1, and named them as PGQD200, PGQD100, PGQD30, PGQD20, PGQD10, and PGQD5, respectively. For comparison, pure PPY and PG10 (PPY/CRGO nanocomposites with the mass ratio of 10:1) were also prepared through the similar procedure[22], to prove that GQD really enhanced the electrochemical properties of PPY as supercapacitor electrode.

In a typical preparation of electrodes, 5 mg sample was pressed into a wafer under a pressure of 2.5 MPa. Then a thin copper wire was connected with the wafer after silver conductive adhesive was painting on it. Additionally, the silver conductive adhesive and the copper wire were covered by a passive layer (Epoxy), to prevent the corrosion of electrolyte.

1.3 Characterization Methods

AFM images of GQD were acquired using a Multimode Nanoscope V scanning probe microscopy (SPM) system (Bruker, USA) in tapping mode. The used AFM cantilever tips are with a force constant of ~ 50 $N \cdot m^{-1}$ and resonance vibration frequency of ~ 350 kHz. Scanning electron microscope (SEM) measurements were carried out by a field emission scanning electron microanalyzer (Zeiss ultra 55, Germany) at an accelerating voltage of 5.0 kV. X-ray diffraction (XRD) data were collected by X-ray powder diffraction (D/max-2600PC, Japan) using Cu K_α radiation (λ = 0.154 178 nm) to identify the structure and species of samples. Fourier transform infrared spectroscopy (FTIR) spectra were measured using an EQUINOX 55 FT-IR spectrometer(Bruker, Germany) by grinding the dried powder of samples and KBr together, and then compressed into thin pellets under 20 MPa.

1.4 Electrochemical Measurements

SZ-82 digital four-point probe system (Suzhou, China) was used to conduct the electrical conductivity measurement of the electrodes. Cyclic voltammetry (CV), galvanostatic charge-discharge, electrochemical impedance spectra (EIS) were measured on a CHI 660C three-electrode electrochemical workstation (Shanghai, China). The electrolyte was 2 $mol \cdot L^{-1}$ H_2SO_4 aqueous solution. An Ag/AgCl electrode and a platinum wire were used as the reference and the counter electrode, respectively. The cyclic voltammetry (CV) response of the electrodes were measured at different scan rates varying from 0.005 $V \cdot s^{-1}$ to 0.1 $V \cdot s^{-1}$ within the potential range of -0.2 to 0.45 V. Galvanostatic charge-discharge was carried out at a current density of 1 $A \cdot g^{-1}$. EIS was collected with the frequency range from 0.01 Hz to 100 kHz.

2 Results and Discussion

2.1 Characterizations

It is well known that the graphene oxide nanosheets contain plenty of hydroxyl, carboxyl, epoxide groups as well as defects on their surfaces when they were prepared through the oxidization and exfoliation of bulk graphite. Those groups and defects can't be fully repaired by reduction, and will surely bring the negative effect to the composites of PPY and CRGO as supercapacitor electrodes, for example cycling stability and conductivity[22]. Therefore, we speculate that quantum dots cut from the graphene oxide nanosheets along the defects by Photo-Fenton reaction will enhance electrochemical performance of polypyrrole. Fig. 1 depicts the typical tapping mode AFM images of the individual GQD, with the diameter of about 50 nm from Fig. 1. The thickness, measured from the height profile of the AFM images, is about 1.0 nm as shown in the inserted image of Fig. 1B.

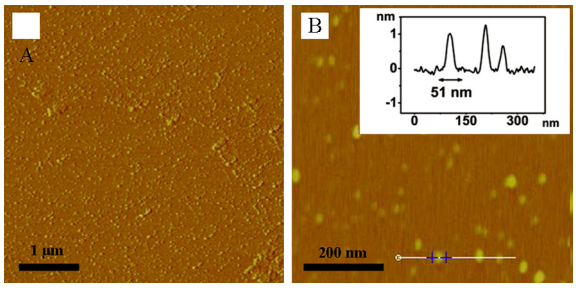

Fig. 1 Tapping-mode AFM images of GQD
A. Phase diagram; B. Height diagram (inserted image is the height profile of the line shown in B)

The PPY/GQD composites were prepared by *in-situ* chemical oxidative polymerization of pyrrole using various concentrations of GQD served as soft template, and the SEM images of pure PPY, PG10, PPY/GQD composites are shown in Fig. 2A ~ D. Due to physical fusing or the crossing polymerization among the particles, we could see a typical PPY spherical morphology with a diameter about 200 nm in Fig. 2A. Although the spherical morphology of the composites is similar to that of the pure PPY, the size of PGQD10 (Fig. 2B) and PGQD50 (Fig. 2C) particles is about 80 nm, much smaller than 200 nm of PPY. Since the original GO used in the work shows unique two dimensional (2D) layered structure [25-26], morphology of PG10 is also layered but thicker, as showed in Fig. 2D. Because the GO has been fully turned into GQD after Photo-Fenton reaction, morphology of PPY/GQD composites is so different from that of PG10. The particles of PGQD50 look like

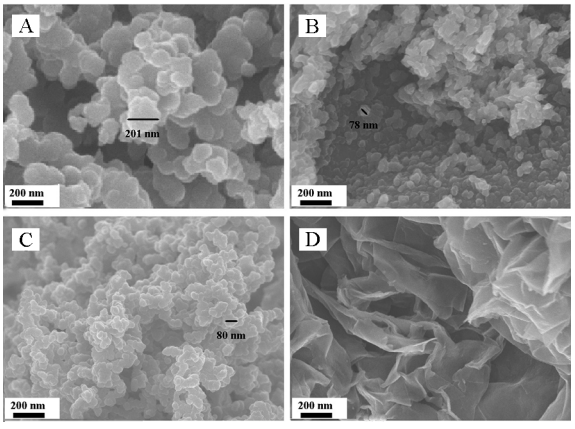

Fig. 2 SEM images of pure PPY (A), PGQD10 (B), PGQD50 (C) and PG10 (D)

more satiated than those of PGQD10. And the morphology of the other PPY/GQD composites is all similar with them. The possible reason is that the ratio of 50:1 happens to be the optimum ratio. When the ratio increased to a certain level, GQD are unable to provide enough templates for growth of pyrrole monomer on them. Therefore, morphology of PPY/GQD composites does not change again. Discussion above implies that PPY was polymerized on the GQD surface.

2.2 XRD and FT-IR Analysis

Fig. 3A shows the XRD patterns of PGQD50 with the diffraction peaks at 2θ = 15.3° and 22.2°. The diffraction peaks at 2θ = 15.3° may be attributed to partial reduction of GQD [27]. The characteristic peak of amorphous for pure PPY appears at about 2θ = 26° [28]. Because of the GQD's adding in the composite, the broad peak shifts from 2θ = 26° to 22.2°, implying that the GQD and PPY have been effectively interacted. The value of interplanar spacing is about 0.39 nm for the broad peak about at 2θ = 22.2°, which is identical to the π-π stacking distance [10]. Therefore, we can believe that there probably exists π-π stacking between the PPY and GQD.

FT-IR spectra of PGQD50 were also acquired and compared with those of pure PPY and GQD, so as to get insight into the interactions between PPY and GQD, showed in Fig. 3B. We can see the typical PPY ring vibrations at 1546 cm^{-1} and 1464 cm^{-1}, the C—N stretching vibration at 1042 cm^{-1} on the FT-IR spectrum of pure PPY [29]. Before the polymerization of the PPY on GQD, the stronger C═O stretching vibration band (1716 cm^{-1}), C═C vibration band (1616 cm^{-1}), and C—O stretching band (1050 cm^{-1}) could be observed on the FT-IR spectrum of the GQD [30]. As the formation of the nanocomposites, for example PGQD50, the aforementioned vibration bands related to the oxygen-containing groups of the GQD disappeared gradually. At the same time, several new bands at 1550, 1470 and 1045 cm^{-1} appeared, which are close to those of the stretching vibrations of pure PPY, but they shifted a little bit to the high wavenumbers. These results indicate that some of the oxygen

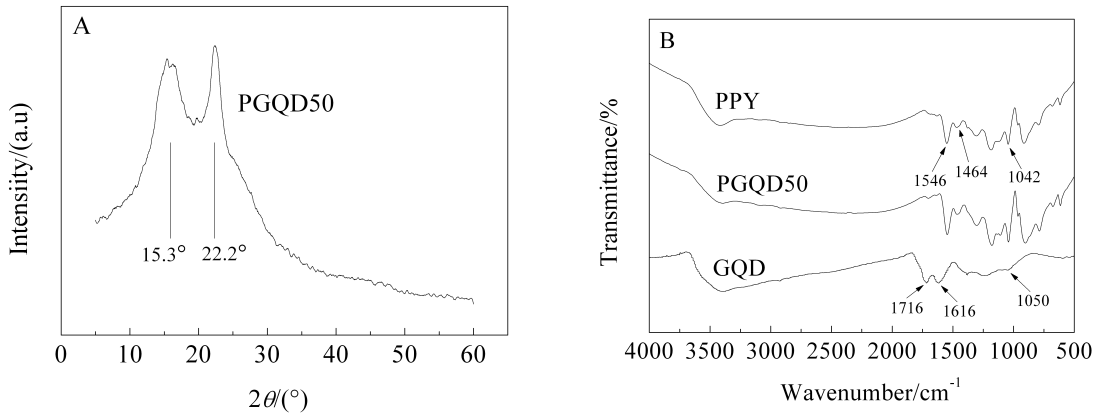

Fig. 3 XRD patterns of PGQD50 (A) and FT-IR spectra of pure PPY, PGQD50 and GQD (B)

containing groups of GQD have been removed, showing that the pyrrole molecule could be used as a reluctant[31]. This result was correspondent with XRD test, and parts of GQD in the composites are reduced. Through characterizations of composites above, PPY and GQD have successfully synthesized together. Thus, we can further use electrochemical testing methods to study this new composite.

2.3 Electrochemical Performance

The electrochemical performance of the samples as the electrode material for supercapacitors was tested by cyclic voltammetry (CV), galvanostatic charge-discharge and electrochemical impedance spectra (EIS) in three-electrode system. The CV curves of different composite electrodes with a potential window from -0.2 to 0.45 V (vs. AgCl/Ag) are shown in Fig. 4A, which are nearly rectangular and symmetric, indicating it is an electrical double-layer capacitor (EDLC). And there exists only a small redox peak at about 0.37 V, illustrating the excellent reversible stability and ideal capacitive behavior of the composites. This small redox peak may be caused by the reduction of the residual oxygen-containing groups in PPY/GQD composites during the electrochemical process at a scan rate of 0.005 V·s^{-1}. The average specific capacitance of the materials is calculated from CV measurements using the following equation:

$$\text{Capacitance}(C_m) = \frac{S}{v\Delta V m} \quad (1)$$

where ΔV is interval between the highest and the lowest scanning voltage, m is the mass of composite in the electrode, S is the area of current-potential curve in CV test, and v is the potential scan rate.

All specific capacitance data of composites under the fifth cycle at a scan rate of 0.005 V·s^{-1} are collected in Tab. 1. The specific capacitance of pure PPY in our work is 344 F·g^{-1}. It can be seen that the PPY/GQD composites with PPY to GQD ratio of 50:1 have the highest specific capacitance of 485 F·g^{-1}. In PGQD5 with specific capacitance of 394 F·g^{-1}, there are lots of GQD and some of them agglutinate together, leading to lower dispersion and specific capacitance. On the other hand, in PGQD200 with specific capacitance of 357 F·g^{-1}, there are fewer GQD and they are unable to provide sufficient templates, leaving the specific capacitance not be improved so much. From the experimental data above, we can see that the composites of GQD and PPY really have a certain synergy. In order to make the materials have the largest capacitance, we need to find the optimal

Tab. 1 List of the specific capacitances of all composites at a scan rate of 0.005 V·s^{-1}

Sample	PGQD5	PGQD10	PGQD20	PGQD30	PGQD50	PGQD100	PGQD200
Capacitance/(F·g^{-1})	394	418	432	455	485	455	357

mass ratio of PPY to GQD. When the mass ratio of PPY/GQD is lower than optimal mass ratio, lots of GQD agglutinate together. When the mass ratio of PPY/GQD is higher than optimal mass ratio, there are not enough templates for PPY growing. Further study of optimal electrode materials showed in Fig. 4.

In Fig. 4A, the larger of the area of current-potential curve, the higher specific capacitance we can get at the same scan rate. Obviously, CV curve of PGQD50 got a larger area, while it reached a higher specific capacitance of 485 $F \cdot g^{-1}$ at a scan rate of 0.005 $V \cdot s^{-1}$. The variation in the specific capacitance of PPY/GQD nanocomposites with different ratios as a function of scan rate is shown in Fig. 4B. It can be seen that the specific capacitances increased as the scan rate decreased in Fig. 4B, and PGQD50 have higher specific capacitance at all different scan rates. The high value of specific capacitance of PGQD50 at a lower scan rate is not only due to the oxidation or deoxidation of α-C or β-C atoms, but also the ions get enough time to migrate freely in PGQD50 matrix[14].

Based on discussion above, we believe PGQD50 is optimal among all PPY/GQD samples, with highest specific capacitance, and its stability is worth looking forward. Fig. 5A shows, as the scan rate increases, the area of CV curves also increases. In addition, the attenuation of the specific capacitance is about 2% after 2000 cycles at a scan rate of 0.05 $V \cdot s^{-1}$, showed in Fig. 5B, indicating it has a good cycling stability. Due might to the further reduction of the residual oxygen-containing groups in PPY/GQD composites during the electrochemical process, an increase of capacitance is observed in the first 100 cycles. A similar phenomenon was reported by others[10]. However, we believe fewer defects in GQD may be the reason why the composites have great cycling stability[24].

In order to compare the capacitances of PPY/GQD composites, PPY/CRGO composites and

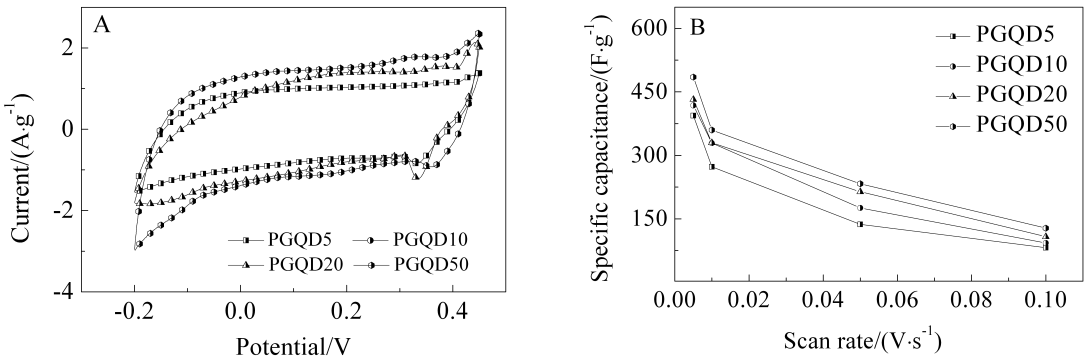

Fig. 4 CV curves at a scan rate of 0.005 $V \cdot s^{-1}$ (A) and the specific capacitances at various scan rates (B) of PGQD5, PGQD10, PGQD20, and PGQD50 electrode

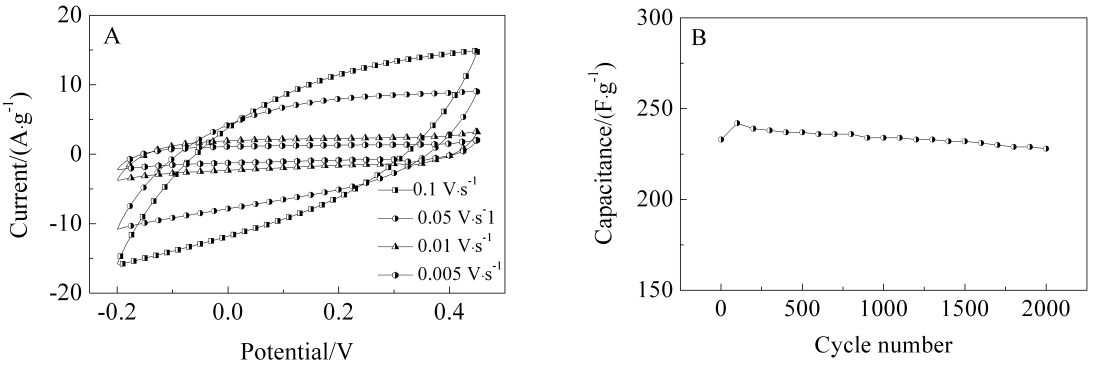

Fig. 5 CV curves at different scan rates (A) and cycling stability at the scan rate of 0.05 $V \cdot s^{-1}$ of PGQD50 (B)

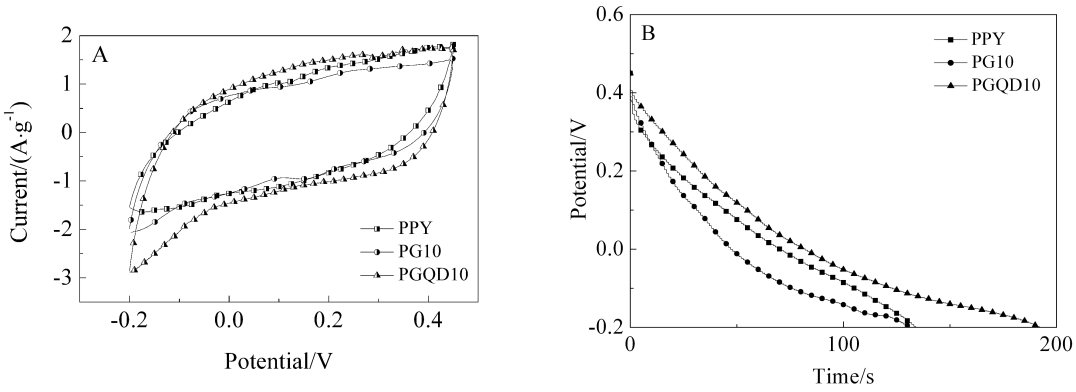

Fig. 6 CV curves at a scan rate of 0.005 V·s^{-1} (A) and Galvanostatic charge-discharge curves at a current density (B) of 1 A·g^{-1} of PPY, PG10 and PGQD10 electrodes

pure PPY, electrochemical tests of pure PPY and PG10 are conducted in the same way. The PG10 have the highest specific capacitance among all PPY/CR-GO samples[22]. Fig. 6A shows the area of CV curve of PGQD10 is larger, which means higher capacitance than PPY and PG10, 344 F·g^{-1} and 340 F·g^{-1}, respectively. Galvanostatic charge-discharge curves obtained at a current density of 1 A·g^{-1}, seen in Fig. 6B. Obviously, the discharging rate of PGQD10 electrode is slower than that of the pure PPY and PG10, indicating it has higher capacitance[22].

Better capacitance performance may be affected by better conductivity. Therefore, EIS and conductivity tests are conducted to prove that PPY/GQD composites have better electrochemical performance. Firstly, the EIS test results of PPY, PG10 and PGQD10 showed in Fig. 7. The impedance plot can be divided into the high frequency and the low frequency component of the plot. In high frequency region, semicircle curve means the electronic transmission between interfaces of electrode materials. On the other hand, the straight part of the plot at lower frequency region inclines more closely to the imaginary axis (*y*-axis), more smoothly the ion diffusion in the electrolyte[32]. We can see PGQD10 electrode's straight part inclines more closely to the imaginary axis in Fig. 7, verifying its better capacitive behavior than other electrodes. The intercept of semicircle at the real axis is the equivalent series resistance (ESR)[33]. From the inserted image of Fig. 7, we got the ESR of PGQD10 electrode is ~ 1.62 Ω, which is smaller than

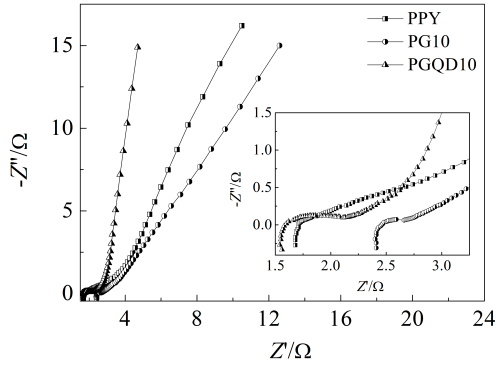

Fig. 7 Nyquist plots of PPY, PG10 and PGQD10 electrodes

any other electrodes, revealing that the PGQD10 electrode assumes shorter ion diffusion path.

The conductivities of these materials further verified discussion above, showed in Tab. 2. The conductivity of PGQD10 is 5.9 S·cm^{-1}, higher than 2.7 S·cm^{-1} of pure PPY and 4.1 S·cm^{-1} of PG10. Due to defects on GO sheets, electronics can't move through GO sheets smoothly, leading to lower conductivity of PG10. Graphene quantum dots got by Photo-Fenton reaction have fewer defects, so PPY/GQD nanocomposites have better conductivity. Conductivity of PGQD50 is higher than PGQD10, also showed in Tab. 2.

Tab. 2 List of conductivities of PPY, PG10, PGQD10 and PGQD50

Sample	PPY	PG10	PGQD10	PGQD50
Conductivity/(S·cm^{-1})	2.7	4.1	5.9	7.2

On the other hand, the morphologies of the electrode materials also have a huge impact on the electrochemical properties and conductivities. For example, the spherical PGQD10 with a diameter about 80 nm, have better electrochemical properties than spherical PPY with a diameter about 200 nm and layered PG10. In the work of Zeng et al, high-quality graphene scrolls (GSS) with a unique scrolled topography were designed and significantly improved electrochemical properties, because of the topological change of graphene sheets[34]. In our experiments, the morphologies of PG10, PGQD10 and PPY changed a lot, leading to their capacitances so different. The smaller particles may have higher specific surface area and increase specific capacitance, such as PGQD and PPY. The layered PG10 provides the broad 2D plane, facilitating ion transport, and thus gets higher capacitance and conductivity than pure PPY. Related in-depth work is undergoing in our group.

Through electrochemical and conductivity test above, we found that PGQD10 have better capacitive behavior, higher conductivity than pure PPY and PG10, which further illustrates that PPY/GQD nanocomposites have better electrochemical performance. Meanwhile, through comparison and tests of a series of PPY/GQD composites, PGQD50 have the optimal electrochemical properties among them. Therefore, PGQD50 are more suitable as supercapacitor electrode materials. All the experimental data above showed that the improved capacitance and enhanced cycling stability of PPY/GQD nanocomposites might be mainly ascribed to fewer defects and smaller particle sizes of composites, which can shorten ion diffusion length and make higher materials utilization.

3 Conclusions

In summary, we demonstrated that PPY could grew on and coated GQD surfaces through *in-situ* polymerization of pyrrole. The PPY/GQD nanocomposites were gained through a simple preparation procedure, which show better electrical conductivity, electrochemical properties and cycling stability than those of individual PPY and PPY/CRGO composites. Morphology and structure of composites are characterized by SEM, XRD and FT-IR, indicating that the nanostructure of PPY was greatly affected by the addition of GQD during the synthesis process. Our results prove that enhanced electrochemical performance can be obtained by doping PPY with a small amount of GQD and the PGQD50 will be a good candidate for supercapacitor electrode with a competitive specific capacitance of 485 $F \cdot g^{-1}$. Further optimization and control of the structures to exploit better electrochemical properties of PPY-based composites are undergoing in our group.

Acknowledgements

This work was supported by the National Natural Science Foundation of China (No. 20906055), National "973 Program" (No. 2010CB933900), and the State key laboratory of bioreactor engineering (No. 2060204). The authors also wish to thank the Instrumental Analysis Center of Shanghai Jiao Tong University.

References:

[1] Zhang K, Zhang L L, Zhao X S, et al. Graphene/polyaniline nanofiber composites as supercapacitor electrodes[J]. Chemistry of Materials, 2010, 22(4): 1392-1401.

[2] Jeong Y U, Manthiram A. Nanocrystalline manganese oxides for electrochemical capacitors with neutral electrolytes[J]. Journal of The Electrochemical Society, 2002, 149(11): A1419-A1422.

[3] Ogihara N, Kawauchi S, Okuda C, et al. Theoretical and experimental analysis of porous electrodes for lithium-ion batteries by electrochemical impedance spectroscopy using a symmetric cell[J]. Journal of The Electrochemical Society, 2012, 159(7): A1034-A1039.

[4] Aravindan V, Chuiling W, Reddy M V, et al. Carbon coated nano-$LiTi_2(PO_4)_3$ electrodes for non-aqueous hybrid supercapacitors [J]. Physical Chemistry Chemical Physics, 2012, 14(16): 5808-5814.

[5] Lazzari M, Mastragostino M, Pandolfo A G, et al. Role of carbon porosity and ion size in the development of Ionic liquid based supercapacitors[J]. Journal of The Electrochemical Society, 2011, 158(1): A22-A25.

[6] Stenger-Smith J D, Guenthner A, Cash J, et al. Poly(propylenedioxy)thiophene-based supercapacitors operating at low temperatures[J]. Journal of The Electrochemical Society, 2010, 157(3): A298-A304.

[7] Bandhauer T M, Garimella S, Fuller T F. A critical review

of thermal issues in lithium-ion batteries[J]. Journal of The Electrochemical Society, 2011, 158(3): R1-R25.

[8] Pandolfo A G, Hollenkamp A F. Carbon properties and their role in supercapacitors[J]. Journal of Power Sources, 2006, 157(1): 11-27.

[9] Winter M, Brodd R J. What are batteries, fuel cells, and supercapacitors? [J]. Chemical Reviews, 2004, 104 (10): 4245-4269.

[10] Zhang D C, Zhang X, Chen Y, et al. Enhanced capacitance and rate capability of graphene/polypyrrole composite as electrode material for supercapacitors[J]. Journal of Power Sources, 2011, 196(14): 5990-5996.

[11] Lufrano F, Staiti P. Performance improvement of Nafion based solid state electrochemical supercapacitor[J]. Electrochimica Acta, 2004, 49(16): 2683-2689.

[12] Simon P, Gogotsi Y. Materials for electrochemical capacitors[J]. Nature Materials, 2008, 7(11): 845-854.

[13] Raymundo-Piñero E, Khomenko V, Frackowiak E, et al. Performance of manganese oxide/CNTs composites as electrode materials for electrochemical capacitors [J]. Journal of The Electrochemical Society, 2005, 152 (1): A229-A235.

[14] Bose S, Kim N H, Kuila T, et al. Electrochemical performance of a graphene-polypyrrole nanocomposite as a supercapacitor electrode[J]. Nanotechnology, 2011, 22(29): 295202-295210.

[15] Vix-Guterl C, Frackowiak E, Jurewicz K, et al. Electrochemical energy storage in ordered porous carbon materials[J]. Carbon, 2005, 43(6): 1293-1302.

[16] Hui Z H, Hong C, Lian L S, et al. The effect of the polyaniline morphology on the performance of polyaniline supercapacitors[J]. Journal of Solid State Electrochemistry, 2005, 9(8): 574-580.

[17] Gupta V, Miura N. High performance electrochemical supercapacitor from electrochemically synthesized nanostructured polyaniline[J]. Materials Letters, 2006, 60(12): 1466-1469.

[18] Ingrama M D, Staeschea H, Ryderb K S. 'Activated' polypyrrole electrodes for high-power supercapacitor applications[J]. Solid State Ionics, 2004, 169(1/4): 51-57.

[19] Sharma R K, Rastogi A C, Desu S B. Pulse polymerized polypyrrole electrodes for high energy density electrochemical supercapacitor[J]. Electrochemistry Communications, 2008, 10(2): 268-272.

[20] Laforgue A, Simon P, Sarrazin C, et al. Polythiophene-based supercapacitors [J]. Journal of Power Sources, 1999, 80(1/2): 142-148.

[21] Geim A K. Graphene: Status and prospects[J]. Science, 2009, 324(5934): 1530-1534.

[22] Xu S Z, Zhou X J, Wu K, et al. Electrochemical performances of layered polypyrrole/chemically reduced graphene oxide nanocomposites as supercapacitor electrodes[J]. Journal of Electrochemistry, 2012, 18(3): 5-16.

[23] Banhart F, Kotakoski J, Krasheninnikov A V. Structural defects in graphene[J]. ACS Nano, 2010, 5(1): 26-41.

[24] Zhou X, Zhang Y, Wang C, et al. Photo-Fenton reaction of graphene oxide: A new strategy to prepare graphene quantum dots for DNA cleavage[J]. ACS Nano, 2012, 6 (8): 6592-6599.

[25] Zhang J L, Yang H J, Shen G X, et al. Reduction of graphene oxide via L-ascorbic acid[J]. Chemical Communications, 2010, 46(7): 1112-1114.

[26] Zhou X J, Zhang J L, Wu H X, et al. Reducing gaphene oide via hdroxylamine: A simple and efficient route to graphene[J]. The Journal of Physical Chemistry C, 2011, 115(24): 11957-11961.

[27] Fan Z, Wang K, Wei T, et al. An environmentally friendly and efficient route for the reduction of graphene oxide by aluminum powder [J]. Carbon, 2010, 48 (5): 1686-1689.

[28] Vishnuvardhan T K, Kulkarni V R, Basavaraja C, et al. Synthesis, characterization and a.c. conductivity of polypyrrole/Y_2O_3 composites[J]. Bulletin of Materials Science, 2006, 29(1): 77-83.

[29] He C, Yang C H, Li Y F. Chemical synthesis of coral-like nanowires and nanowire networks of conducting polypyrrole[J]. Synthetic Metals, 2003, 139(2): 539-545.

[30] Peng J, Gao W, Gupta B K, et al. Graphene quantum dots derived from carbon fibers[J]. Nano Letters, 2012, 12(2): 844-849.

[31] Amarnath C A, Hong C E, Kim N H, et al. Efficient synthesis of graphene sheets using pyrrole as a reducing agent[J]. Carbon, 2011, 49(11): 3497-3502.

[32] Conway B E. Electrochemical supercapacitors: Scientific fundamentals and technological applications[M]. Springer, 1999: 444-445.

[33] Ramasamy R P, Ramadass P, Haran B S, et al. Synthesis, characterization and cycling performance of novel chromium oxide cathode materials for lithium batteries [J]. Journal of Power Sources, 2003, 124(1): 155-162.

[34] Zeng F, Kuang Y, Liu G, et al. Supercapacitors based on high-quality graphene scrolls[J]. Nanoscale, 2012, 4(13): 3997-4001.

石墨烯量子点增强聚吡咯超级电容器电极的电化学性质

吴 坤, 许思哲, 周雪皎, 吴海霞*

(上海交通大学微纳科学技术研究院, 上海 200240)

摘要: 通过将吡咯单体在低温下与石墨烯量子点进行原位聚合, 获得一种全新的聚吡咯/石墨烯量子点(PPY/GQD)复合材料. 实验中采用了扫描电子显微镜(SEM)、原子力显微镜(AFM)、X 射线衍射(XRD)、红外光谱(FT-IR)和热重分析(TGA)对复合物的表面形貌、结构进行表征. 结果表明, 吡咯单体以石墨烯量子点为软模板, 以化学键的方式在石墨烯量子点的表面聚合生长成片状聚吡咯. 通过机械冷压法将粉末状 PPY/GQD 复合物压成圆片电极. 电极的电化学测试结果表明, PPY 和 GQD 质量比为 50:1 所制得的复合物的电容量为 485 $F \cdot g^{-1}$, 同时在 2000 次循环之后电容量只降低了大约 2%. 通过与同比例的 PG(聚吡咯/石墨烯复合材料)以及纯 PPY 对比, 发现聚吡咯/石墨烯量子点的高比容量及优异的循环稳定性将会使其在电化学超级电容器领域中具有潜在的应用价值.

关键词: 氧化石墨烯; 石墨烯量子点; 聚吡咯; 超级电容器